Arabian Journal of Chemistry (2020) 13, 1120–1129

King Saud University

Arabian Journal of Chemistry

www.ksu.edu.sa
www.sciencedirect.com

ORIGINAL ARTICLE

Synthesis and biological evaluation of novel coumarin-chalcone derivatives containing urea moiety as potential anticancer agents

Belma Zengin Kurt [a], Nur Ozten Kandas [b], Aydan Dag [a], Fatih Sonmez [c,*], Mustafa Kucukislamoglu [c]

[a] *Bezmialem Vakif University, Faculty of Pharmacy, Department of Pharmaceutical Chemistry, 34093 Istanbul, Turkey*
[b] *Bezmialem Vakif University, Faculty of Pharmacy, Department of Pharmaceutical Toxicology, 34093 Istanbul, Turkey*
[c] *Sakarya University, Faculty of Arts and Science, Department of Chemistry, 54055 Sakarya, Turkey*

Received 12 July 2017; accepted 1 October 2017
Available online 7 October 2017

KEYWORDS

Coumarin;
Chalcone;
Urea;
Hepatoma;
Antitumor;
Cytotoxicity;
Cell-cycle;
Apoptosis

Abstract The increasing interest on new drug discovery is constantly up to date as drugs do not increase survival adequately against increasing cancer cases worldwide. Based on the reported anticancer activity of coumarin, chalcone and urea derivatives, the present investigation dealt with the design and synthesis of coumarin derivatives bearing diversely substituted chalcone-urea moieties **5a-k**. Through a structure-based molecular hybridization approach, a series of novel coumarin-chalcone derivatives containing urea moiety was synthesized and screened for their *in vitro* antiproliferative activities against the cancer cell lines (H4IIE and HepG2). In addition, the synthesized compounds were tested on a cell line that was not cancerous (CHO) and the damage, it could give to normal cells was determined. Among the synthesized compounds, **5k** exhibited better inhibition of H4IIE compared to Sorafenib. **5j** also showed better inhibition against HepG2 than Sorafenib. In particular, **5k** induced H4IIE apoptosis, arrested cell cycle at the S phase. Therefore, **5k** and **5j** may be potent antitumor agents, representing a promising lead for further optimization.
© 2017 The Authors. Production and hosting by Elsevier B.V. on behalf of King Saud University. This is an open access article under the CC BY-NC-ND license (http://creativecommons.org/licenses/by-nc-nd/4.0/).

1. Introduction

Hepatoma or Hepatocellular carcinoma (HCC) is one of the most common malignancies throughout the world with a high incidence and mortality which occurs predominantly in patients with underlying chronic liver disease and cirrhosis (Yang et al., 2014; Lin et al., 2015). HCC is the third leading reason among cancer-related death reasons worldwide, with a calculated incidence of more than 600,000 new cases annually (Liu et al., 2013). The present treatment of HCC, including

* Corresponding author.
E-mail address: fsonmez@sakarya.edu.tr (F. Sonmez).
Peer review under responsibility of King Saud University.

Production and hosting by Elsevier

https://doi.org/10.1016/j.arabjc.2017.10.001
1878-5352 © 2017 The Authors. Production and hosting by Elsevier B.V. on behalf of King Saud University.
This is an open access article under the CC BY-NC-ND license (http://creativecommons.org/licenses/by-nc-nd/4.0/).

surgical resection and chemoembolization, cannot take a significant effect on HCC, except for liver transplantation, therefore the use of chemotherapeutic agents are limited (OuYang et al., 2013; Zhang et al., 2014). Consequently, development of new chemotherapeutic agents has great significance.

Coumarin (1,2H-chromen-2-one or 2H-1-benzopyran-2-one) is a bicyclic heterocycle compound, consisting of benzene and 2-pyrone rings. Coumarins are also a wide class of natural and synthetic compounds that showed versatile pharmacological activities (Sashidhara et al., 2013; Emami and Dadashpour, 2015), such as anti-inflammatory (Fylaktakidou et al., 2004), antioxidant (Kostova et al., 2011), hepatoprotective (Atmaca et al., 2011), antithrombotic (Peng et al., 2013), antiviral (Curini et al., 2003), antimicrobial (Ostrov et al., 2007), antituberculosis (Manvar et al., 2011), anticarcinogenic (Basanagouda et al., 2014), antihyperlipidemic (Yuce et al., 2009), monoamine oxidase-B inhibitors (Hammuda et al., 2016) and anticholinesterase (Kurt et al., 2015) activities.

Chalcones (1,3-diaryl-2-propen-1-ones) consist of two aromatic rings connected by an α,β-unsaturated carbonyl group, belonging to the flavonoid class of natural products. They have drawn considerable amount of interest because of their pharmacological properties and their synthetic derivatives having a significant cytotoxic activity against various cancer cells (Pingaew et al., 2014; Mai et al., 2014; Mahapatra et al., 2015). Chalcones also exhibited many various biological and pharmacological activities, such as antibacterial (Liaras et al., 2011), antimalarial (Larsen et al., 2005), antifungal (Lahtchev et al., 2008), antiviral (Cheenpracha et al., 2006), anti-inflammatory (Wu et al., 2003), antimicrobial (Mobinikhaledi et al., 2012) and anticancer effects (Sashidhara et al., 2010).

Urea derivatives, especially bis-aryl ureas, are one of the well-known class among the anticancer agents, because of their strong inhibitory activities against receptor tyrosine kinases (RTKs), Raf kinases, protein tyrosine kinases (PTKs) (Zhan et al., 2012), vascular endothelial growth factor receptor (VEGF), platelet-derived growth factor receptor (PDGFRB) (Liu et al., 2014) and NADH oxidase. Sorafenib and similar diaryl-urea derivatives have promoted synthesis of new urea derivatives because of their high antiproliferative activity (Lu et al., 2014; Chen et al., 2016).

In this study, we designed and synthesized a series of novel coumarin-chalcone containing urea derivatives, with the aim of acquiring agents displaying more potent antitumor activities. Antitumor effects of the newly synthesized compounds were investigated on the *in vitro* growth of H4IIE (rat hepatoma), HepG2 (human hepatocellular carcinoma) and CHO (Chinese hamster ovary) cell lines. Sorafenib was used as a positive control.

2. Experimental

2.1. Material and method

Melting points were determined on a Barnstead Electrothermal 9200. IR spectra were measured on Alfa Bruker spectrometer. ^{1}H and ^{13}C NMR spectra were measured on a Varian Infinity Plus spectrometer at 300 and at 75 Hz, respectively. ^{1}H and ^{13}C chemical shifts are referenced to the internal deuterated solvent. Mass spectra were obtained using MICROMASS Quattro LC-MS-MS spectrometer. The elemental analyses were carried out with a Leco CHNS-932 instrument. LDH cell cytotoxicity was recorded using microplate reader (Bio-Rad model 550; Bio-Rad Laboratories, Hercules, CA). For flow cytometric analysis Muse® Cell Analyzer was used. The cell line and kits were purchased from Sigma (Steinheim, Germany) and American Type Culture Collection (ATCC). The other chemicals and solvents were purchased from Fluka Chemie, Merck, Alfa Easer and Sigma-Aldrich. Dulbecco's Modified Eagle's Medium-F12, fetal calf serum, and PBS Dulbecco's without calcium, magnesium, and sodium bicarbonate were purchased from GIBCO BRL, InVitrogen (Carlsbad, CA). Muse Annexin V and Dead Cell Kit (Cat# MCH100105) and Muse Cell Cycle Kit (Cat# MCH100106) were purchased from (Millipore, USA). MTT and Cytotoxicity Detection Kit (LDH) were obtained from Roche Life Sciences. In all studies, concentrated substances were filtered and diluted in DMSO to different concentrations immediately before use.

2.2. General procedures of synthesis and spectral data

2.2.1. 3-acetyl-2H-chromen-2-one (2)

A mixture of benzaldehyde (**1**) (3 mmol), ethylacetoacetate (3 mmol), and piperidine (0.3 mol) was stirred at room temperature for 15 min. The mixture was filtered and the precipitated product was recrystallized from ethanol. **2** was obtained in 85% yields. Spectral data of this compound was matched with the literature (Sonmez et al., 2017).

2.2.2. 3-(3-(4-Nitrophenyl)acryloyl)-2H-chromen-2-one (3)

3-Acetylcoumarin (**2**) (0.01 mol) and p-nitrobenzaldehyde (0.01 mol) were dissolved in absolute ethanol (50 mL) and catalytic amount of piperidine (0.001 mol) was added and it was stirred for 10 min at room temperature. The mixture was refluxed for 6 h and then it was cooled. The precipitated product was filtered, washed with cold ethanol and dried in air. It was recrystallized from ethanol. Spectral data of this compound was matched with the literature (Patel et al., 2014).

2.2.3. 3-(3-(4-Aminophenyl)acryloyl)-2H-chromen-2-one (4)

The coumarin-nitrochalcone (**3**) (1 mmol) was dissolved in 50 mL of absolute ethanol, and $SnCl_2{\cdot}2H_2O$ (5 mmol) was added in this solution. The mixture was refluxed for 2 h. It was cooled and ethanol was evaporated. Then it was neutralized with aqueous $NaHCO_3$ solution (30 mL). The mixture was extracted with 3 × 50 mL of EtOAc. The combined organic phase was dried with $MgSO_4$, filtered, and evaporated. The residue was purified by chromatography on silica gel with Hexane/EtOAc as eluant (4:1) (Sonmez et al., 2011). Red powder, 62% yield; mp. 250–252 °C; IR: 3333, 3216, 3040, 1717, 1557, 1509, 1444, 1299, 1163, 979, 820, 752, 510 cm^{-1}; ^{1}H NMR (DMSO-d_6, 300 MHz) δ/ppm: 6.12 (2H, d, J = 6.7 Hz), 6.60 (2H, s), 6.88 (2H, s, br), 7.12–7.78 (6H, m), 8.56 (1H, s); ^{13}C NMR (DMSO-d_6, 75 MHz) δ/ppm: 114.0, 116.8, 118.2, 125.0, 125.4, 127.9, 128.8, 129.6, 129.8, 134.2, 142.0, 147.2, 147.6, 153.2, 159.2, 188.6.

2.3. General procedure for the synthesis of 1-(substituted)-3-(4-(3-oxo-3-(2-oxo-2H-chromen-3-yl)prop-1-en-1-yl)phenyl)urea (5a-k) derivatives

A mixture of isocyanate derivative (1 mmol) and **4** in THF (30 mL) containing triethyl amine (1.2 mmol) was heated under reflux for overnight. The solution was evaporated and the residue was washed with 10 mL of EtOAc. The precipitated product was filtered and dried in a vacuum-oven.

*2.3.1. 1-(3-Methoxyphenyl)-3-(4-(3-oxo-3-(2-oxo-2H-chromen-3-yl)prop-1-en-1-yl)phenyl)urea (**5a**)*

Orange powder, 78% yield; mp. 226–228 °C; IR: 3262, 3040, 1711, 1664, 1590, 1523, 1415, 1312, 1223, 1166, 985, 824, 753, 631 cm^{-1}; ^1H NMR (DMSO-d_6, 300 MHz) δ/ppm: 3.73 (3H, s), 6.57 (1H, dd, J = 2.0, 7.9 Hz), 6.95 (1H, d, J = 8.2 Hz), 7.16–7.22 (2H, m), 7.41–7.57 (5H, m), 7.69–7.77 (4H, m), 7.94 (1H, dd, J = 1.4, 7.9 Hz), 8.65 (1H, s), 8.79 (1H, s, NH), 9.01 (1H, s, NH); ^{13}C NMR (DMSO-d_6, 75 MHz) δ/ppm: 55.6, 104.7, 108.1, 111.3, 116.9, 118.7, 119.1, 122.9, 125.6, 126.4, 128.5, 130.3, 130.7, 131.0, 134.7, 141.2, 143.1, 145.1, 147.2, 152.8, 155.0, 159.1, 160.3, 187.8. LC-MS (m/z): 439.3[M^+]. Anal. Calcd. for $C_{26}H_{20}N_2O_5$; C, 70.90; H, 4.58; N, 6.36; found: 70.92; H, 4.56; N, 6.30.

*2.3.2. 1-(4-Methoxyphenyl)-3-(4-(3-oxo-3-(2-oxo-2H-chromen-3-yl)prop-1-en-1-yl)phenyl)urea (**5b**)*

Orange powder, 82% yield; mp. 229–231 °C; IR: 3309, 3040, 1715, 1656, 1591, 1505, 1410, 1312, 1225, 1173, 984, 826, 752, 515 cm^{-1}; ^1H NMR (DMSO-d_6, 300 MHz) δ/ppm: 3.72 (3H, s), 6.87 (2H, d, J = 8.4 Hz), 7.36 (2H, d, J = 8.2 Hz), 7.43–7.56 (5H, m), 7.68–7.75 (4H, m), 7.94 (1H, d, J = 7.9 Hz), 7.98 (1H, s), 8.64 (1H, s, NH), 8.95 (1H, s, NH); ^{13}C NMR (DMSO-d_6, 75 MHz) δ/ppm: not determined; LC-MS (m/z): 439.3[M^+]. Anal. Calcd. for $C_{26}H_{20}N_2O_5$; C, 70.90; H, 4.58; N, 6.36; found: 70.94; H, 4.58; N, 6.28.

*2.3.3. 1-(3-Fluorophenyl)-3-(4-(3-oxo-3-(2-oxo-2H-chromen-3-yl)prop-1-en-1-yl)phenyl)urea (**5c**)*

Orange powder, 62% yield; mp. 259–261 °C; IR: 3385, 3037, 1714, 1687, 1552, 1514, 1444, 1310, 1173, 994, 824, 750, 616 cm^{-1}; ^1H NMR (DMSO-d_6, 300 MHz) δ/ppm: 6.79 (2H, d, J = 8.4 Hz), 7.12 (1H, d, J = 8.2 Hz), 7.27–7.35 (1H, m), 7.40–7.56 (5H, m), 7.69–7.77 (4H, m), 7.93 (1H, d, J = 7.9 Hz), 8.64 (1H, s), 9.01 (1H, s, NH), 9.09 (1H, s, NH); ^{13}C NMR (DMSO-d_6, 75 MHz) δ/ppm: 105.5, 105.8, 114.7, 116.8, 118.8, 119.1, 123.1, 125.6, 126.4, 128.7, 130.6, 131.0, 134.7, 141.8, 142.0, 142.9, 145.0, 147.2, 152.7, 155.0, 159.1, 161.4, 187.8. LC-MS (m/z): 427.3 [M^+]. Anal. Calcd. for $C_{25}H_{17}FN_2O_4$; C, 70.09; H, 4.00; N, 6.54; found: C, 70.12; H, 4.05; N, 6.50.

*2.3.4. 1-(4-Fluorophenyl)-3-(4-(3-oxo-3-(2-oxo-2H-chromen-3-yl)prop-1-en-1-yl)phenyl)urea (**5d**)*

Orange powder, 66% yield; mp. 261–262 °C; IR: 3305, 3041, 1714, 1664, 1568, 1504, 1314, 1212, 1172, 983, 827, 755, 510 cm^{-1}; ^1H NMR (DMSO-d_6, 300 MHz) δ/ppm: 7.13 (2H, d, J = 8.7 Hz), 7.41–7.57 (7H, m), 7.69–7.77 (4H, m), 7.94 (1H, d, J = 7.9 Hz), 8.64 (1H, s), 8.91 (1H, s, NH), 9.12 (1H, s, NH); ^{13}C NMR (DMSO-d_6, 75 MHz) δ/ppm: not determined; LC-MS (m/z): 427.3 [M^+]. Anal. Calcd. for $C_{25}H_{17}FN_2O_4$; C, 70.09; H, 4.00; N, 6.54; found: C, 70.11; H, 4.04; N, 6.52.

*2.3.5. 1-(3-Chlorophenyl)-3-(4-(3-oxo-3-(2-oxo-2H-chromen-3-yl)prop-1-en-1-yl)phenyl)urea (**5e**)*

Orange powder, 74% yield; mp. 257–259 °C; IR: 3393, 3038, 1704, 1687, 1599, 1513, 1309, 1176, 996, 823, 744, 574 cm^{-1}; ^1H NMR (DMSO-d_6, 300 MHz) δ/ppm: 7.06 (1H, d, J = 7.6 Hz), 7.29–7.31 (2H, m), 7.43–7.57 (6H, m), 7.70–7.75 (4H, m), 7.94 (1H, d, J = 7.0 Hz), 8.64 (1H, s), 8.99 (1H, s, NH), 9.10 (1H, s, NH); ^{13}C NMR (DMSO-d_6, 75 MHz) δ/ppm: 116.8, 117.5, 118.6, 118.9, 119.1, 122.4, 123.1, 125.6, 126.4, 128.7, 130.6, 131.0, 131.1, 133.9, 134.7, 141.6, 142.9, 145.0, 147.2, 152.7, 155.0, 159.1, 187.8. LC-MS (m/z): 443.3 [M^+]. Anal. Calcd. for; $C_{25}H_{17}ClN_2O_4$; C, 67.50; H, 3.85; N, 6.30; found: C, 67.54; H, 3.83; N, 6.31.

*2.3.6. 1-(4-Chlorophenyl)-3-(4-(3-oxo-3-(2-oxo-2H-chromen-3-yl)prop-1-en-1-yl)phenyl)urea (**5f**)*

Orange powder, 42% yield; mp. 268–269 °C; IR: 3310, 3040, 1695, 1660, 1600, 1516, 1308, 1210, 1170, 981, 822, 751, 455 cm^{-1}; ^1H NMR (DMSO-d_6, 300 MHz) δ/ppm: 7.32–7.35 (2H, m), 7.41–7.57 (7H, m), 7.69–7.75 (4H, m), 7.94 (1H, dd, J = 1.4, 7.6 Hz), 8.65 (1H, s), 8.94 (1H, s, NH), 9.08 (1H, s, NH); ^{13}C NMR (DMSO-d_6, 75 MHz) δ/ppm: not determined; LC-MS (m/z): 443.3 [M^+]. Anal. Calcd. for; $C_{25}H_{17}ClN_2O_4$; C, 67.50; H, 3.85; N, 6.30; found: C, 67.55; H, 3.82; N, 6.32.

*2.3.7. 1-(4-Bromophenyl)-3-(4-(3-oxo-3-(2-oxo-2H-chromen-3-yl)prop-1-en-1-yl)phenyl)urea (**5g**)*

Red powder, 64% yield; mp. 277–279 °C; IR: 3298, 3040, 1706, 1661, 1566, 1514, 1308, 1222, 1168, 980, 819, 750, 503 cm^{-1}; ^1H NMR (DMSO-d_6, 300 MHz) δ/ppm: 7.41–7.58 (9H, m), 7.69–7.78 (4H, m), 7.94 (1H, dd, J = 1.4, 7.9 Hz), 8.65 (1H, s), 8.93 (1H, s, NH), 9.07 (1H, s, NH); ^{13}C NMR (DMSO-d_6, 75 MHz) δ/ppm: 114.3, 116.8, 118.8, 119.1, 120.9, 123.0, 125.6, 126.4, 128.6, 130.6, 131.0, 132.2, 134.7, 139.5, 143.0, 145.1, 147.2, 152.7, 155.0, 159.1, 187.8. LC-MS (m/z): 513.3 [M^+]. Anal. Calcd. for; $C_{25}H_{17}BrN_2O_4$; C, 61.36; H, 3.50; N, 5.72; found: C, 61.34; H, 3.52; N, 5.70.

*2.3.8. 1-(4-Iodophenyl)-3-(4-(3-oxo-3-(2-oxo-2H-chromen-3-yl)prop-1-en-1-yl)phenyl)urea (**5h**)*

Orange powder, 48% yield; mp. 281–283 °C; IR: 3301, 3039, 1707, 1678, 1568, 1514, 1310, 1224, 1173, 983, 819, 747, 576 cm^{-1}; ^1H NMR (DMSO-d_6, 300 MHz) δ/ppm: 7.28–7.33 (3H, m), 7.41–7.58 (7H, m), 7.60–7.78 (3H, m), 7.94 (1H, d, J = 7.3 Hz), 8.65 (1H, s), 8.91 (1H, s, NH), 9.07 (1H, s, NH); ^{13}C NMR (DMSO-d_6, 75 MHz) δ/ppm: 85.7, 116.8, 118.8, 119.1, 121.2, 121.2, 123.0, 125.6, 126.4, 128.6, 130.6, 131.0, 134.7, 138.0, 138.0, 140.0, 143.0, 145.1, 147.2, 152.7, 155.0, 159.1, 187.8. LC-MS (m/z): 559.2 [M^+]. Anal. Calcd. for; $C_{25}H_{17}IN_2O_4$; C, 55.99; H, 3.19; N, 5.22; found: C, 55.96; H, 3.17; N, 5.25.

*2.3.9. 1-(4-(3-oxo-3-(2-oxo-2H-chromen-3-yl)prop-1-en-1-yl)phenyl)-3-phenylurea (**5i**)*

Red powder, 74% yield; mp. 259–261 °C; IR: 3296, 3036, 1705, 1677, 1566, 1513, 1309, 1227, 1169, 980, 823, 746, 572 cm^{-1}; ^1H NMR (DMSO-d_6, 300 MHz) δ/ppm: 6.99 (1H, t, J = 7.0

Hz), 7.27–7.31 (2H, m), 7.45–7.57 (7H, m), 7.70–7.75 (4H, m), 7.94 (1H, d, J = 7.0 Hz), 8.64 (1H, s), 8.77 (1H, s, NH), 9.02 (1H, s, NH); ^{13}C NMR (DMSO-d_6, 75 MHz) δ/ppm: 116.8, 118.7, 119.0, 122.8, 123.0, 125.6, 126.4, 128.4, 129.5, 130.6, 131.0, 134.7, 140.0, 143.2, 145.1, 147.2, 152.8, 155.0, 159.1, 187.8. LC-MS (m/z): 409.3 [M$^+$]. Anal. Calcd. for; $C_{25}H_{18}N_2O_4$; C, 73.16; H, 4.42; N, 6.83; found: C, 73.14; H, 4.45; N, 6.81.

2.3.10. 1-(4-Nitrophenyl)-3-(4-(3-oxo-3-(2-oxo-2H-chromen-3-yl)prop-1-en-1-yl)phenyl)urea (**5j**)

Red powder, 80% yield; mp. 265–266 °C; IR: 3361, 3040, 1702, 1688, 1600, 1500, 1309, 1170, 1109, 983, 825, 753, 576 cm^{-1}; ^{1}H NMR (DMSO-d_6, 300 MHz) δ/ppm: 7.41–7.60 (5H, m), 7.69–7.75 (6H, m), 7.94 (1H, d, J = 7.0 Hz), 8.20 (2H, d, J = 9.0 Hz), 8.65 (1H, s), 9.29 (1H, s, NH), 9.56 (1H, s, NH); ^{13}C NMR (DMSO-d_6, 75 MHz) δ/ppm: 92.6, 116.9, 118.3, 118.6, 119.1, 123.4, 125.6, 125.8, 126.4, 129.1, 130.6, 131.0, 134.7, 141.9, 142.4, 144.9, 146.7, 147.3, 149.3, 152.4, 155.0, 159.1, 187.8. LC-MS (m/z): 478.3 [M$^+$]. Anal. Calcd. for; $C_{25}H_{17}N_3O_6$; C, 65.93; H, 3.76; N, 9.23; found: C, 65.95; H, 3.74; N, 9.24.

2.3.11. 1-(4-(3-Oxo-3-(2-oxo-2H-chromen-3-yl)prop-1-en-1-yl)phenyl)-3-(4(trifluoromethyl) phenyl)urea (**5k**)

Orange powder, 66% yield; mp. 290–291 °C; IR: 3302, 3040, 1707, 1682, 1568, 1516, 1408, 1323, 1173, 1105, 984, 827, 752, 581 cm^{-1}; ^{1}H NMR (DMSO-d_6, 300 MHz) δ/ppm: 7.41–7.48 (2H, m), 7.51–7.76 (11H, m), 7.94 (1H, d, J = 7.6 Hz), 8.65 (1H, s), 9.16 (1H, s, NH), 9.21 (1H, s, NH); ^{13}C NMR (DMSO-d_6, 75 MHz) δ/ppm: 116.8, 118.7, 118.9, 119.1, 123.1, 125.6, 126.3, 126.7, 128.8, 130.6, 131.0, 134.7, 142.7, 144.9, 147.3, 152.6, 155.0, 159.1, 187.7. LC-MS (m/z): 501.3 [M$^+$]. Anal. Calcd. for; $C_{26}H_{17}F_3N_2O_4$; C, 65.27; H, 3.58; N, 5.86; found: C, 65.23; H, 3.59; N, 5.88.

2.4. Biological activities

2.4.1. Cell culture and treatments

HII4E rat hepatoma, HepG2 human hepatocellular carcinoma and Chinese hamster ovary (CHO) cells were obtained from ATCC® CRL1548™. All cell lines were cultured in DMEM/F12 with L-glutamine supplemented with 10% FBS, and 100 IU/ml penicillin and 100 μg/ml streptomycin at 37 °C in a humidified atmosphere of 5% CO_2 in air. Cells were cultured in T75 or T25 flasks unless stated otherwise, and the medium was changed when cells reached 50–75% confluence.

In order to determine the nontoxic maximum dose and still maintain the viability of the cells HII4E rat hepatoma cells, HepG2 human hepatocellular carcinoma and Chinese hamster ovary (CHO) cells were treated with 11 different substances in the concentration ranges of 0–100 μM. According to the trypan blue assay, 0.625 μM, 1.25 μM, 2.5 μM, 5 μM, 10 μM, 20 μM, 40 μM, 80 μM and 160 μM doses were picked to assess cell cytotoxicity, cell cycle and apoptosis assays.

2.4.2. Cell viability/cytotoxicity assays

To determine the effect of substances on cell proliferation and cell viability by hemocytometer counting, cells were plated onto 24-well cell culture plates at 5000 cells/well in 1 mL of culture medium with FBS. Before treatment cells were allowed to adhere to the bottom of the plate for 24 h and treated with different concentrations of substances. At 24 h treatment at 37 °C, the cells were harvested by trypsin solution. Cell counts were performed in triplicates using a hemocytometer with trypan blue (0.2%) exclusion to identify viable cells. The total numbers of viable and dye-stained cells in each experiment were compared with those of the parallel untreated control cell counts performed simultaneously in three independent experiments.

Two methods were used to determine the cytotoxic effects of the synthesized compounds. For the LDH cell cytotoxicity (Smith et al., 2011) assay, cells were seeded in 96-well plates (5000 cells/well) and treated with substances for 24 h. LDH (Lactate dehydrogenase) solution was added as 10 μL to each well and incubated for an additional period of 3–5 h at 37 °C in a humidified incubator and the absorbance at 520 nm was recorded using microplate reader (Bio-Rad model 550; Bio-Rad Laboratories, Hercules, CA). This method was used to determine the effects of the synthesized compounds on rat hepatoma cells (HII4E).

The second method, MTT, was used to determine the effects of the synthesized compounds on HepG2 and CHO cells. The cytotoxicity effects of tested compounds were evaluated by MTT assay according to described method (Kurt et al., 2017). Briefly MTT assay, cells were seeded in a flat-bottomed 96-well plate at a density of 5 × 104 cells/well in DMEM/F12 containing 10% FBS. The plate was incubated at 37 °C with 5% CO_2 for 24 h, and then compounds were prepared and added to make a final concentration of 160, 80, 40, 20, 10, 5, 2.5, 1.25, 0.625 μM, respectively, in serum-free DMEM/F12. Cells were further incubated for 24 h at 37 °C with 5% CO_2; then, the medium was replaced with DMEM/F12 containing 10% FBS. 10 μL of filter-sterilized MTT (3-(4,5 dimethylthia zol-2-yl)-2,5-diphenyltetrazolium bromide) solution (5 mg/mL in PBS) was added to each well and further incubated at 37 °C with 5% CO_2 for 4 h. At the end of incubation media was aspirated from the wells and 100 μL of DMSO was added to dissolve insoluble formosan crystals formed. The absorbance was measured at 570 nm using a microtiter plate reader.

2.4.3. Cell cycle distribution and apoptosis

Muse® Cell Analyzer was used for flow cytometric analysis. Both cell cycle distribution and apoptotic cells were simultaneously measured in Muse® Cell Analyzer (Merck Millipore) according to the manufacturer‘s protocol (Khan et al., 2012).

3. Results and discussions

3.1. Design and synthesis

Modification of the natural compounds is used to develop new anticancer agents. Many studies on coumarin-chalcone hybrid derivatives have emphasized that these groups have good anticancer properties (Perez-Cruz et al., 2013; Pingaew et al., 2014; Wei et al., 2016). The diaryl urea and amide groups, as key pharmacophores, possess a unique binding mode and kinase inhibition profile. The design and development of novel bioactive materials incorporating the integration of two or more pharmacophore units with different mechanisms of action within the same molecule are rationally attractive, based on

the molecular hybridization strategy (Vazquez-Rodriguez et al., 2015). Hybridization of these pharmacophore groups offers some advantages such as coming from the top of the probable drug resistance and at the same time increasing their biological potential (Pingaew et al., 2014). Based on this approach, it is believed that the coumarin-chalcone compounds containing the urea group can significantly inhibit cell proliferation (Fig.1).

The synthetic procedures to obtain the target compounds **5a-k** are depicted in Scheme 1. 3-acetylcoumarin (**2**) was synthesized from salicylaldehyde (**1**) according to the literature (Sonmez et al., 2017), then it was reacted with *p*-nitrobenzaldehyde in ethanol. 3-(3-(4-aminophenyl)acryloyl)-2H-chromen-2-one (**4**) was obtained by reducing 3-(3-(4-nitro phenyl)acryloyl)-2H-chromen-2-one (**3**) with $SnCl_2{\cdot}H_2O$ Coumaryl-chalcone substituted urea derivatives (**5a-k**) were obtained by the reacting **4** with various isocyanate derivatives in THF.

Numerous methods have been developed for the synthesis of coumarin derivatives, including the Pechmann condensation, the Perkin reaction, the Knoevenagel condensation, the Wittig reaction, and the Baylis–Hillman reaction (Vekariya and Patel, 2014). However, the Pechmann and the Knoevenagel reactions are widely useful for the synthesis of coumarins with simple reaction conditions and good yield of the products. On the other hand, a lot of methods have been reported for the synthesis of chalcone derivatives such as Aldol condensation, Claisen-Schmidt condensation, Suzuki reaction, Witting reaction, Friedel-Crafts acylation with cinnamoyl chloride, Photo-Fries rearrangement of phenyl cinnamates etc. Among them, Aldol condensation and Claisen-Schmidt condensation are still the most used methods (Bukhari et al., 2012). There are many studies to invent and develop the known methods and techniques for the synthesis of both coumarin and chalcone derivatives. They utilize various catalysts and reagents in different solvents or solvent-free (Bigi et al., 1999; Bukhari et al., 2012; Vekariya and Patel, 2014; Maleki et al., 2016; Maleki et al., 2017; Maleki and Azadegan, 2017a,b). In this study, the Knoevenagel condensation and Claisen-Schmidt condensation were preferred for the synthesis of coumarin-chalcone scaffold, respectively. This scaffold (compound **3**) was obtained in mild conditions (solvent-free and room temperature in first step) and in high yields. Consequently, the invention or the development of the new techniques was not considered in these steps.

In third step, tin chlorine was used as a reducing agent. Metal salts are used as a catalyst in many synthetic methods. Among them, tin salts, especially $SnCl_2$, are often used in the

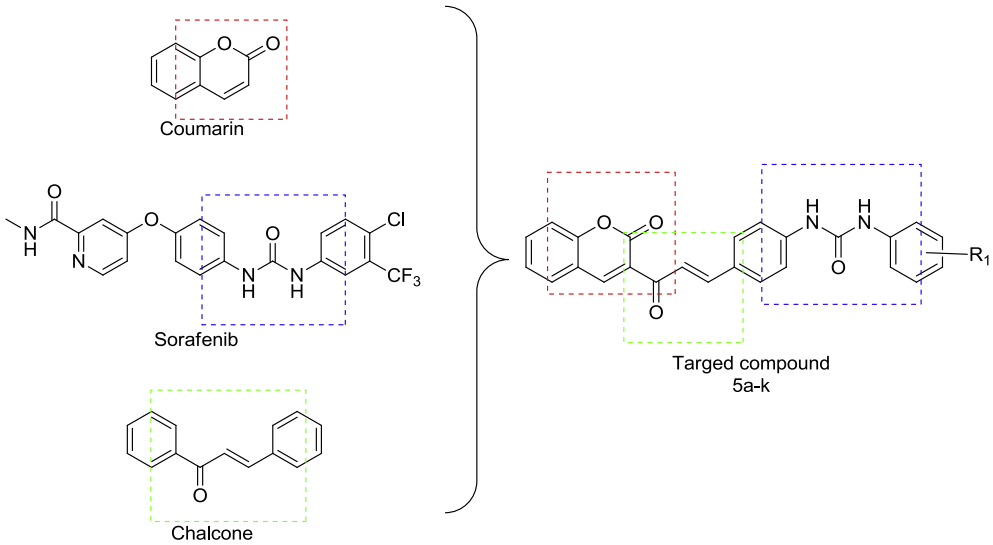

Fig. 1 Design strategy of the targeted compounds.

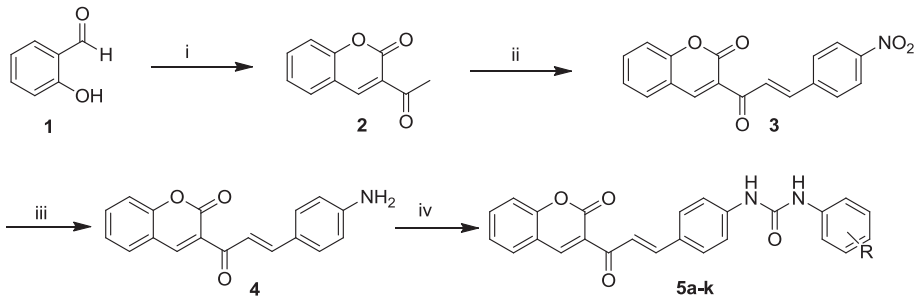

Scheme 1 Synthesis of new coumaryl-chalcone substituted urea derivatives. Reaction conditions: (i) Ethylacetoacetate, piperidin, rt; (ii) *p*-nitrobenzaldehyde, piperidin, EtOH, 80 °C, 6h, (iii) $SnCl_2x2H_2O$, EtOH, 80 °C, 2h, (iv) R-phenylisocyanate, Et_3N, THF, 70 °C, overnight.

reduction of nitroarenes (Chicha et al., 2013), synthesis of pyridine derivatives (Reddy et al., 2015) and β-amino ketones (Alanthadka et al., 2017), one-pot synthesis of indazole (Sudhapriya et al., 2017) and indol-quinoline (Fan et al., 2017) etc. as a reducing agent. $SnCl_2$, a safe and inexpensive reagent, is usually preferred for reduction reactions due to its ease of operation and the purity of the obtained products, in non-aqueous conditions (Bellamy and Ou, 1984). Furthermore, the mild conditions and the selectivity of this reduction method are one of the reasons of its preference. The yield ranges different values according to the structures of the compounds. For example, the reduction of isoxazoloquinoline with $SnCl_2$ was occurred in almost 20% yields (Madapa et al., 2007). In another study, the nitro group was reduced in 80% yields for the synthesis of imidazole (Ermann et al., 2002). The reduction of a nitro group on the indazole was performed using $SnCl_2$ in moderate yields (Abbassi et al., 2011). The reduction of nitrochalcone derivative was obtained in 60% yields using $SnCl_2$ as a catalyst in this study. $SnCl_2$ selectively reduces aromatic nitro compounds under nonacidic and non-aqueous conditions through deoxygenation of the nitro compound to amine compound (Gottlieb et al., 2000). The $SnCl_2$ converts to SnO_2 at the end of the reaction. Water-insoluble SnO_2 precipitating during the extraction can be removed by filtration (Grunewald et al., 1983).

All the new compounds were characterized by ^{1}H NMR, ^{13}C NMR, IR, MS and elemental analysis. ^{1}H NMR, ^{13}C NMR, and MS spectra of the synthesized compounds are given in supplementary materials. In the infrared spectra of the synthesized compounds, it was possible to observe the absorptions between 3370 and 3250 cm^{-1} relating to NH stretch for urea derivatives, about 1700 cm^{-1} from chalcone carbonyl moiety stretch, absorptions between 1600 and 1690 cm^{-1} from coumarin and urea carbonyl moiety stretching. From the ^{1}H NMR spectra, the resonance due to the hydrogen attached to the amide nitrogen was between 8.60 and 9.56 ppm. The signals for aromatic hydrogens were observed between 6.90 and 8.69 ppm. From the ^{13}C NMR spectra, the signals of carbonyl groups can be seen at 187 ppm, 159 ppm and 155 ppm, relating to chalcone, coumarin and urea moieties, respectively. The signals of aromatic carbons can also be seen between 105–150 ppm.

3.2. Biological activities

3.2.1. Cell cytotoxicity

The cytotoxicity of the coumarin-chalcone derivatives against H4IIE, HepG2 and CHO were evaluated. The ability of these diarylureas to inhibit the growth of cancer cells was summarized in Table 1.

The majority of the synthesized compounds displayed potent antitumor activity against H4IIE and HepG2 cells. Among them, **5 k**, having trifluoromethyl group at the *para*-position of phenyl ring, and **5j**, having nitro at the *para*- position of phenyl ring, exhibited the most potent activity with IC_{50} values of 1.62 and 2.326 μM, respectively. The synthesized compounds were also tested on healthy cell lines such as cancerous cell lines. The results showed that they had less influence on healthy cells than cancerous cells; on the other hand they were more effective than Sorafenib on cancer cells and normal cells.

3.2.2. Structure-activity relationship

The following results of the structure-activity relationship should be noted regarding the cytotoxicity activities of the synthesized compounds (**5a-k**) against H4IIE and HepG2 cells:

For H4IIE; (i) moving the methoxy group and chloro atom at the phenyl ring from the *meta*-position to the *para*-position led to a decline of the cytotoxicity activities (compare **5a** (R = 3-OMe, IC_{50} = 9.37 μM) with **5b** (R = 4-OMe, IC_{50} = 14.66 μM) and compare **5e** (R = 3-Cl, IC_{50} = 2.07 μM) with **5f** (R = 4-Cl, IC_{50} = 2.83 μM)); (ii) moving the fluoro atom at the phenyl ring from the *meta*-position to the *para*-position led to an increase of the cytotoxicity activities (compare **5c** (R = 3-F, IC_{50} = 19.78 μM) with **5d** (R = 4-F, IC_{50} = 8.67 μM)); (iii) electron-donating groups (methoxy) at the *para*- positions of the phenyl ring exhibited lower cyto-

Table 1 Cytotoxicity (IC_{50}, μM) activities of the synthesized compounds (5a-k) against H4IIE, HepG2 and CHO cells *in vitro*.

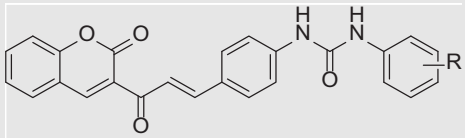

Compound	R	H4IIE (IC_{50}, μM)[a]	HepG2 (IC_{50}, μM)[a]	CHO (IC_{50}, μM)[a]
5a	3-OCH_3	9.37 ± 1.25	6.052 ± 0.66	28.456 ± 2.84
5b	4-OCH_3	14.66 ± 0.88	11.172 ± 1.19	18.240 ± 2.37
5c	3-F	19.78 ± 1.57	11.298 ± 1.11	28.664 ± 4.01
5d	4-F	8.67 ± 1.33	11.427 ± 1.71	25.016 ± 3.25
5e	3-Cl	2.07 ± 0.79	8.518 ± 1.02	14.051 ± 1.68
5f	4-Cl	2.83 ± 0.98	6.064 ± 0.72	19.878 ± 2.78
5g	4-Br	3.33 ± 1.12	8.564 ± 0.84	3.824 ± 2.24
5h	4-I	2.23 ± 1.05	9.020 ± 1.08	19.168 ± 2.68
5i	4-H	15.73 ± 1.25	7.153 ± 0.71	21.552 ± 2.80
5j	4-NO_2	13.06 ± 1.44	2.326 ± 0.23	23.208 ± 2.55
5k	4-CF_3	1.62 ± 0.57	8.212 ± 1.14	21.490 ± 3.22
Sorafenib	–	3.45 ± 0.68	7.522 ± 1.05	20.188 ± 3.02

[a] Results are expressed as means ± SD (standard deviation) of four independent experiments.

toxicity activity compared to electron-withdrawing groups (nitro and trifluoromethyl) (compare **5b** (R = 4-OMe, IC_{50} = 14.66 μM) with **5j** (R = 4-NO_2, IC_{50} = 13.06 μM) and **5 k** (R = 4-CF_3, IC_{50} = 1.62 μM); (iv) the cytotoxicity activity against H4IIE cells seems to be related with the size and polarizability of the halogen substituent at the *para*-position of the phenyl ring (for size and polarizability, I > Cl > F; **5 h** (R = 4-I, IC_{50} = 2.23 μM) > **5f** (R = 4-Cl, IC_{50} = 2.83 μM) > **5d** (R = 4-F, IC_{50} = 8.67 μM); however, this relation did not match for **5 g** (R = 4-Br, IC_{50} = 3.33 μM).

For HepG2; (i) moving the methoxy group at the phenyl ring from the *meta*-position to the *para*-position led to a decline of the cytotoxicity activities (compare **5a** (R = 3-OMe, IC_{50} = 6.052 μM) with **5b** (R = 4-OMe, IC_{50} = 11.172 μM); (ii) moving the fluoro atom at the phenyl ring from the *meta*-position to the *para*-position led to the same of the cytotoxicity activities (compare **5c** (R = 3-F, IC_{50} = 11.298 μM) with **5d** (R = 4-F, IC_{50} = 11.427 μM); (iii) electron-donating groups (methoxy) at the *para*- positions of the phenyl ring exhibited lower cytotoxicity activity compared to electron-withdrawing groups (nitro and trifluoromethyl) (compare **5b** (R = 4-OMe, IC_{50} = 11.172 μM) with **5j** (R = 4-NO_2, IC_{50} = 2.326 μM) and **5 k** (R = 4-CF_3, IC_{50} = 8.212 μM); (iv) the cytotoxicity activity against HepG2 cells seems to be related with the size and polarizability of the halogen substituent at the *para*-position of the phenyl ring (for size and polarizability, Cl > Br > I; **5f** (R = 4-Cl, IC_{50} = 6.064 μM) > **5 g** (R = 4-Br, IC_{50} = 8.564 μM) > **5 h** (R = 4-I, IC_{50} = 9.020 μM); however, this relation did not match for **5d** (R = 4-F, IC_{50} = 11.427 μM).

Table 2 Effects of compound 5e, 5f, 5g, 5h and 5k on cell cycle progression in H4IIE cells.

Compound	Conc. (μM)	G1/G0 (%)	S (%)	G2/M (%)
Sorafenib	10	38.2 ± 1.25	42.7 ± 2.05	15.8 ± 0.88
5e	10	5.3 ± 0.88	50.3 ± 1.36	32.5 ± 1.24
5f	10	28.4 ± 0.96	46.4 ± 1.42	15.3 ± 1.22
5 g	10	8.1 ± 1.02	42.2 ± 0.69	32.9 ± 0.58
5 h	10	22.8 ± 2.55	31.8 ± 0.74	31.3 ± 0.32
5 k	10	24.2 ± 2.14	47.8 ± 1.82	20.8 ± 1.23

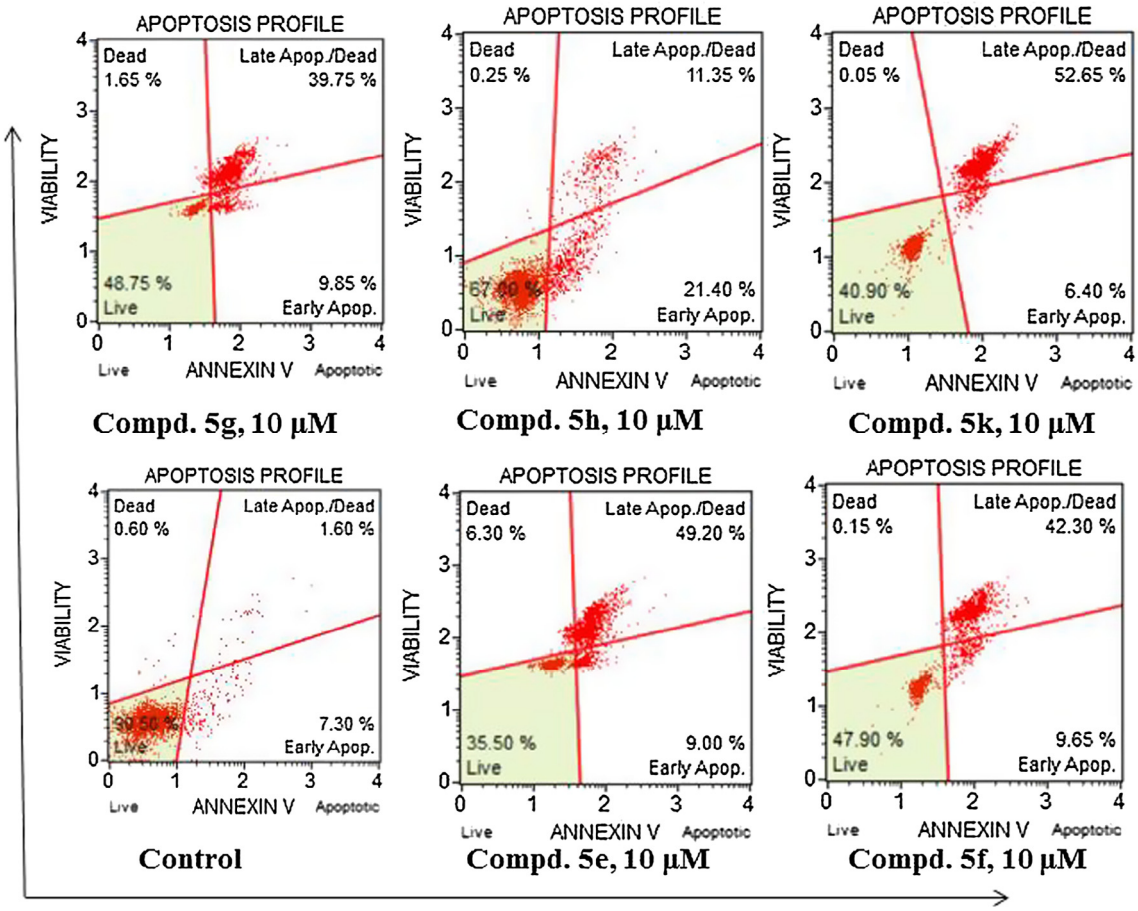

Fig. 2 Effect of **5e**, **5f**, **5g**, **5h** and **5k** on the induction of apoptosis in H4IIE cells.

According to the results of test on the CHO cell line (Table 1), **5a** (R = 3-OMe, IC_{50} = 28.456 μM) and **5c** (R = 4-F, IC_{50} = 28.664 μM) showed the lowest toxicity. These values are lower than those of the Sorafenib (IC_{50} = 20.188 μM). **5 g** (R = 4-Br, IC_{50} = 3.824 μM) showed higher toxicity compared to other compounds. In general, most of the compounds showed less toxicity than Sorafenib on CHO cell line.

3.2.3. Cell cycle distribution

The cell cycle distribution in H4IIE cells was examined to determine inhibition effects of compound **5e**, **5f**, **5g**, **5h** and **5k** on the proliferation of these cells through cell cycle arrest. In generally, cell cycle analysis demonstrated that compounds treatment concentration increased the population of cells in the S phase. As shown in Table 2, the population of H4IIE cells in the S phase increased to 50.3% after treatment with 10 μM of compound **5e** for 24 h. In addition, S phase blockage increased to 47.8, 46.4, 42.2 and 31.8%, after treatment with 10 μM of compound **5k**, **5f**, **5g**, **5h** for 24 h, respectively. These data indicated that cell cycle arrest in the S stage contributed to the antiproliferative effects of compound **5e**, **5f**, **5g**, **5h** and **5k** on H4IIE cells.

3.2.4. Apoptosis

The appearance of phosphatidylserine (PS) residue of the cell that is normally hidden within the plasma membrane on the surface indicates an early event in apoptosis and can be used to detect and measure apoptosis. PS is translocated from the cytoplasmic face of the plasma membrane to the cell surface during apoptosis. Annexin V has a strong Ca^{2+}-dependent affinity for PS and therefore can be used as a probe for detecting apoptosis. For the quantitative analysis of live, early and late apoptosis on cells, the Muse™ Cell Analyzer was used. Control group have 90.50% live cells while Early Apoptosis cells percentage is 7.30% and Late Apoptosis cells percentage is 1.60% in Fig. 2.

Having the best cytotoxic effect **5k** caused 59% apoptosis. There was also a similarity between the cytotoxic effects of other compounds and apoptosis results. According to these results; compounds **5e**, **5f** and **5g** provided apoptosis in 58%, 51% and 49%, respectively. **5h** had the cytotoxic effect with IC_{50} value of 2.23 μM, but it led to apoptosis of 32% of the H4IIE cells. Generally, the synthesized substances can be said to lead to controlled death of H4IIE cells.

The octanol/water partition coefficient, logP, is one of the most important physico chemical parameters for the development of new anticancer drugs with improved pharmacokinetic properties. LogP is one of the properties identified by Lipinski in the "Rule of 5″ for drug-like molecules, and is therefore, one of the most important physicochemical parameters in drug discovery studies, being related to the bioavailability of chemical compounds (Tetko et al., 2016). The ACD/ ChemSketch software (ACD/ChemSketch 4.0) predicts physicochemical properties based on the assumption that these properties can be estimated using additive atomic or group increments (Osterberg and Norinder, 2001). We calculated the logP values of synthesized compounds and sorafenib using the ACD/ ChemSketch program, in this study. The obtained results are given in Table 3. It was determined that the logP values of the compounds synthesized according to these results were similar to the sorafenib compound.

Table 3 LogP values of the synthesized coumaryl-chalcone substituted urea derivatives.

Compound	Log P[a]
5a	4.98 ± 0.75
5b	4.67 ± 0.75
5c	5.20 ± 0.75
5d	5.16 ± 0.75
5e	5.75 ± 0.75
5f	5.71 ± 0.75
5g	5.88 ± 0.75
5h	6.14 ± 0.75
5i	4.72 ± 0.75
5j	5.17 ± 0.75
5k	5.73 ± 0.75
Sorafenib	5.16 ± 0.75

[a] Logp calculated from ChemSketch ACD labs 2012.

4. Conclusions

In summary a series of novel coumarin-chalcone containing urea derivatives was synthesized and tested for their antiproliferative activities against H4IIE and HepG2 cancer cell lines. Among them, five compounds (**5e**, **5f**, **5g**, **5h** and **5k**) exhibited stronger activities than Sorbenib against a H4IIE cancer cell line. The effects of the synthesized compounds on apoptosis and cell cycle were also investigated to elucidate the mechanism of anticancer action. Most of them stopped cell cycle in phase S. Although the cell cycle was stopped in phase S, the active compounds were found to induce apoptosis of the cancer cell. Especially **5k** and **5e** have the best apoptosis and cytotoxicity activity. On the other hand, compounds **5a**, **5f** and **5j** showed better inhibition against HepG2 cells than Sorafenib. All of the synthesized compounds (except **5g**) were found to have similar effects with the sorafenib according to the results of test on the normal cell line. The synthesized compounds inhibited the proliferation of cancer cells, but they did not show such an effect on the normal cell line at the same concentration. The lipophilic properties of the synthesized compounds were determined by calculating the logo values, one of the pharmacokinetic properties. This study may provide valuable information for future design and development of antitumor agents with more potent activities.

Acknowledgments

This work was supported by the Sakarya Research Fund of the Sakarya University. Project Number: 2016-28-00-003.

Appendix A. Supplementary material

Supplementary data associated with this article can be found, in the online version, at https://doi.org/10.1016/j.arabjc.2017.10.001.

References

Abbassi, N., Rakib, E.M., Bouissane, L., Hannioui, A., Khouili, M., El Malki, A., Benchidmi, M., Essassi, E.M., 2011. Studies on the

reduction of the nitro group in 4-nitroindazoles by anhydrous SnCl2 in different alcohols. Synth. Commun. 41, 999–1005.

Alanthadka, A., Devi, E.S., Selvi, A.T., Nagarajan, S., Sridharan, V., Maheswari, C.U., 2017. N-heterocyclic carbene-catalyzed mannich reaction for the synthesis of beta-amino ketones: N, N-dimethylformamide as carbon source. Adv. Synth. Catal. 359, 2369–2374.

Atmaca, M., Bilgin, H.M., Obay, B.D., Diken, H., Kelle, M., Kale, E., 2011. The hepatoprotective effect of coumarin and coumarin derivates on carbon tetrachloride-induced hepatic injury by antioxidative activities in rats. J. Physiol. Biochem. 67, 569–576.

Basanagouda, M., Jambagi, V.B., Barigidad, N.N., Laxmeshwar, S.S., Devaru, V., Narayanachar, 2014. Synthesis, structure-activity relationship of iodinated-4-aryloxymethyl-coumarins as potential anti-cancer and anti-mycobacterial agents. Eur. J. Med. Chem. 74, 225–233.

Bellamy, F.D., Ou, K., 1984. Selective reduction of aromatic nitrocompounds with stannous chloride in non-acidic and non-aqueous medium. Tetrahedron Lett. 25, 839–842.

Bigi, F., Chesini, L., Maggi, R., Sartori, G., 1999. Montmorillonite KSF as an ınorganic, water stable, and reusable catalyst for the knoevenagel synthesis of coumarin-3-carboxylic acids. J. Org. Chem. 64, 1033–1035.

Bukhari, S.N.A., Malina, J., Jantan, I., 2012. Synthesis and biological evaluation of chalcone derivatives. Mini Rev. Med. Chem. 12, 1394–1403.

Cheenpracha, S., Karalai, C., Ponglimanont, C., Subhadhirasakul, S., Tewtrakul, S., 2006. Anti-HIV-1 protease activity of compounds from Boesenbergia pandurata. Bioorg. Med. Chem. 14, 1710–1714.

Chen, J.N., Wang, X.F., Li, T., Wu, D.W., Fu, X.B., Zhang, G.J., Shen, X.C., Wang, H.S., 2016. Design, synthesis, and biological evaluation of novel quinazolinyl-diaryl urea derivatives as potential anticancer agents. Eur. J. Med. Chem. 107, 12–25.

Chicha, H., Abbassi, N., Rakib, E., Khouili, M., El Ammari, L., Spinelli, D., 2013. Reduction of 3-nitrophthalic anhydride by SnCl2 in different alcohols: a simple synthesis of alkyl 1,3-dihydro-3-oxo-2,1-benzisoxazole-4-carboxylates. Tetrahedron Lett. 54, 1569–1571.

Curini, M., Epifano, F., Maltese, F., Marcotullio, M.C., Gonzales, S. P., Rodriguez, J.C., 2003. Synthesis of collinin, an antiviral coumarin. Aust. J. Chem. 56, 59–60.

Emami, S., Dadashpour, S., 2015. Current developments of coumarin-based anti-cancer agents in medicinal chemistry. Eur. J. Med. Chem. 102, 611–630.

Ermann, M., Simkovsky, N.M., Roberts, S.M., Parry, D.M., Baxter, A.D., 2002. Solid-phase synthesis of imidazo[4,5-b]pyridin-2-ones and related urea derivatives by cyclative cleavage of a carbamate linkage. J. Comb. Chem. 4, 352–358.

Fan, L., Liu, M., Ye, Y., Yin, G., 2017. Synthesis of 6-substituted 6H-Indolo[2,3-b]quinolines from Isoindigos. Org. Lett. 19, 186–189.

Fylaktakidou, K.C., Hadjipavlou-Litina, D.J., Litinas, K.E., Nicolaides, D.N., 2004. Natural and synthetic coumarin derivatives with anti-inflammatory/antioxidant activities. Curr. Pharm. Design. 10, 3813–3833.

Gottlieb, L., Hassner, A., Gottlieb, H.E., 2000. Stannous chloride reduction of nitroalkenes in amines. Synthesis and cycloaddition of α- dialkylaminoaldoxime. Synth. Commun. 30, 2445–2464.

Grunewald, G.L., Paradkar, V.M., Pazhenchevsky, B., Pleiss, M.A., Sall, D.J., Seibel, W.L., Reitz, T.J., 1983. Conformationally defined adrenergic agents. 8. Synthesis of conformationally defined analogs of norfenfluramine - a highly stereospecific synthesis of amines from alcohols in the Benzobicyclo[2.2.1]Heptene System. J. Org. Chem. 48, 2321–2327.

Hammuda, A., Shalaby, R., Rovida, S., Edmondson, D.E., Binda, C., Khalil, A., 2016. Design and synthesis of novel chalcones as potent selective monoamine oxidase-B inhibitors. Eur. J. Med. Chem. 114, 162–169.

Khan, A., Gillis, K., Clor, J., Tyagarajan, K., 2012. Simplified evaluation of apoptosis using the Muse cell analyzer. Postepy. Biochem. 58, 492–496.

Kostova, I., Bhatia, S., Grigorov, P., Balkansky, S., Parmar, V.S., Prasad, A.K., Saso, L., 2011. Coumarins as antioxidants. Curr. Med. Chem. 18, 3929–3951.

Kurt, B.Z., Gazioglu, I., Sonmez, F., Kucukislamoglu, M., 2015. Synthesis, antioxidant and anticholinesterase activities of novel coumarylthiazole derivatives. Bioorg. Chem. 59, 80–90.

Kurt, B.Z., Gazioglu, I., Dag, A., Salmas, R.E., Kayik, G., Durdagi, S., Sonmez, F., 2017. Synthesis, anticholinesterase activity and molecular modeling study of novel carbamate-substituted thymol/carvacrol derivatives. Bioorg. Med. Chem. 25, 1352–1363.

Lahtchev, K.L., Batovska, D.I., Parushev, S.P., Ubiyvovk, V.M., Sibirny, A.A., 2008. Antifungal activity of chalcones: a mechanistic study using various yeast strains. Eur. J. Med. Chem. 43, 2220–2228.

Larsen, M., Kromann, H., Kharazmi, A., Nielsen, S.F., 2005. Conformationally restricted anti-plasmodial chalcones. Bioorg. Med. Chem. Lett. 15, 4858–4861.

Liaras, K., Geronikaki, A., Glamoclija, J., Ciric, A., Sokovic, M., 2011. Thiazole-based chalcones as potent antimicrobial agents. Synthesis and biological evaluation. Bioorg. Med. Chem. 19, 3135–3140.

Lin, W.L., Lai, D.Y., Lee, Y.J., Chen, N.F., Tseng, T.H., 2015. Antitumor progression potential of morusin suppressing STAT3 and NF kappa B in human hepatoma SK-Hep1 cells. Toxicol. Lett. 232, 490–498.

Liu, Y.Y., Wang, W., Fang, B., Ma, F.Y., Zheng, Q., Deng, P.Y., Zhao, S.S., Chen, M.J., Yang, G.X., He, G.Y., 2013. Anti-tumor effect of germacrone on human hepatoma cell lines through inducing G2/M cell cycle arrest and promoting apoptosis. Eur. J. Pharmacol. 698, 95–102.

Liu, Z.J., Wang, Y., Lin, H.F., Zuo, D.Z., Wang, L.H., Zhao, Y.F., Wang, L.H., Zhao, Y.F., Gong, P., 2014. Design, synthesis and biological evaluation of novel thieno[3,2-d] pyrimidine derivatives containing diaryl urea moiety as potent antitumor agents. Eur. J. Med. Chem. 85, 215–227.

Lu, C.S., Tang, K., Li, Y., Li, P., Lin, Z.Y., Yin, D.L., Chen, X.G., Huang, H.H., 2014. Design, synthesis and evaluation of novel diaryl urea derivatives as potential antitumor agents. Eur. J. Med. Chem. 77, 351–360.

Madapa, S., Sridhar, D., Yadav, G.P., Maulik, P.R., Batra, S., 2007. A general approach to the synthesis of substituted isoxazolo[4,3-c] quinolines via chalcones. Eur. J. Org. Chem., 4343–4351

Mahapatra, D.M., Bharti, S.K., Asati, V., 2015. Anti-cancer chalcones: structural and molecular target perspectives. Eur. J. Med. Chem. 98, 69–114.

Mai, C.W., Yaeghoobi, M., Abd-Rahman, N., Kang, Y.B., Pichika, M.R., 2014. Chalcones with electron-withdrawing and electron-donating substituents: anticancer activity against TRAIL resistant cancer cells, structure-activity relationship analysis and regulation of apoptotic proteins. Eur. J. Med. Chem. 77, 378–387.

Maleki, A., Azadegan, S., 2017a. Amine-Functionalized silica-supported magnetic nanoparticles: preparation, characterization and catalytic performance in the chromene synthesis. J. Inorg. Organomet. P 27, 714–719.

Maleki, A., Azadegan, S., 2017b. Preparation and characterization of silica-supported magnetic nanocatalyst and application in the synthesis of 2-amino-4H-chromene-3-carbonitrile derivatives. Inorg. Nano-Met. Chem. 47, 917–924.

Maleki, A., Movahed, H., Ravaghi, P., Kari, T., 2016. Facile in situ synthesis and characterization of a novel PANI/Fe3O4/Ag nanocomposite and investigation of catalytic applications. Rsc Adv. 6, 98777–98787.

Maleki, A., Movahed, H., Ravaghi, P., 2017. Magnetic cellulose/Ag as a novel eco-friendly nanobiocomposite to catalyze synthesis of chromene-linked nicotinonitriles. Carbohyd. Polym. 156, 259–267.

Manvar, A., Bavishi, A., Radadiya, A., Patel, J., Vora, V., Dodia, N., Rawal, K., Shah, A., 2011. Diversity oriented design of various hydrazides and their in vitro evaluation against Mycobacterium tuberculosis H37(Rv) strains. Bioorg. Med. Chem. Lett. 21, 4728–4731.

Mobinikhaledi, A., Kalhor, M., Jamalifar, H., 2012. Synthesis, characterization and antimicrobial activities of some novel bis-chalcones. Med. Chem. Res. 21, 1811–1816.

Osterberg, T., Norinder, U., 2001. Prediction of drug transport processes using simple parameters and PLS statistics - the use of ACD/logP and ACD/ChemSketch descriptors. Eur. J. Pharm. Sci. 12, 327–337.

Ostrov, D.A., Prada, J.A.H., Corsino, P.E., Finton, K.A., Le, N., Rowe, T.C., 2007. Discovery of novel DNA gyrase inhibitors by high-throughput virtual screening. Antimicrob. Agents. Chem. 51, 3688–3698.

OuYang, F.J., Wang, G.B., Guo, W., Zhang, Y.Y., Xiang, W.H., Zhao, M., 2013. AKT signalling and mitochondrial pathways are involved in mushroom polysaccharide-induced apoptosis and G(1) or S phase arrest in human hepatoma cells. Food Chem. 138, 2130–2139.

Patel, J., Dholariya, H., Patel, K., Bhatt, J., Patel, K., 2014. Cu(II) and Ni(II) complexes of coumarin derivatives with fourth generation flouroquinolone: synthesis, characterization, microbicidal and antioxidant assay. Med. Chem. Res. 23, 3714–3724.

Peng, X.M., Damu, G.L.V., Zhou, C.H., 2013. Current developments of coumarin compounds in medicinal chemistry. Curr. Pharm. Des. 19, 3884–3930.

Perez-Cruz, F., Vazquez-Rodriguez, S., Matos, M.J., Herrera-Morales, A., Villamena, F.A., Das, A., Gopalakrishnan, B., Olea-Azar, C., Santana, L., Uriarte, E., 2013. Synthesis and electrochemical and biological studies of novel coumarin- chalcone hybrid compounds. J. Med. Chem. 56, 6136–6145.

Pingaew, R., Saekee, A., Mandi, P., Nantasenamat, C., Prachayasittikul, S., Ruchirawat, S., Prachayasittikul, V., 2014. Synthesis, biological evaluation and molecular docking of novel chalcone-coumarin hybrids as anticancer and antimalarial agents. Eur. J. Med. Chem. 85, 65–76.

Reddy, D.N.K., Chandrasekhar, K.B., Ganesh, Y.S.S., Kumar, B.S., Adepu, R., Pal, M., 2015. SnCl2 center dot 2H(2)O as a precatalyst in MCR: synthesis of pyridine derivatives via a 4-component reaction in water. Tetrahedron Lett. 56, 4586–4589.

Sashidhara, K.V., Kumar, A., Kumar, M., Sarkar, J., Sinha, S., 2010. Synthesis and in vitro evaluation of novel coumarin-chalcone hybrids as potential anticancer agents. Bioorg. Med. Chem. Lett. 20, 7205–7211.

Sashidhara, K.V., Palnati, G.R., Sonkar, R., Avula, S.R., Awasthi, C., Bhatia, G., 2013. Coumarin chalcone fibrates: a new structural class of lipid lowering agents. Eur. J. Med. Chem. 64, 422–431.

Smith, S.M., Wunder, M.B., Norris, D.A., Shellman, Y.G., 2011. A Simple Protocol for Using a LDH-Based Cytotoxicity Assay to Assess the Effects of Death and Growth Inhibition at the Same Time. Plos One 6.

Sonmez, F., Kurt, B.Z., Gazioglu, I., Basile, L., Dag, A., Cappello, V., Ginex, T., Kucukislamoglu, M., Guccione, S., 2017. Design, synthesis and docking study of novel coumarin ligands as potential selective acetylcholinesterase inhibitors. J. Enzym. Inhib. Med. Ch 32, 285–297.

Sonmez, F., Sevmezler, S., Atahan, A., Ceylan, M., Demir, D., Gencer, N., Arslan, O., Kucukislamoglu, M., 2011. Evaluation of new chalcone derivatives as polyphenol oxidase inhibitors. Bioorg. Med. Chem. Let. 21, 7479–7482.

Sudhapriya, N., Balachandran, C., Awale, S., Perumal, P.T., 2017. Sn (II)-Mediated facile approach for the synthesis of 2-aryl-2H-indazole-3-phosphonates and their anticancer activities. New. J. Chem. 41, 5582–5594.

Tetko, I.V., Varbanov, H.P., Galanski, M., Talmaciu, M., Platts, J.A., Ravera, M., Gabano, E., 2016. Prediction of logP for Pt(II) and Pt (IV) complexes: comparison of statistical and quantum-chemistry based approaches. J. Inorg. Biochem. 156, 1–13.

Vazquez-Rodriguez, S., Lopez, R.L., Matos, M.J., Armesto-Quintas, G., Serra, S., Uriarte, E., Santana, L., Borges, F., Crego, A.M., Santos, Y., 2015. Design, synthesis and antibacterial study of new potent and selective coumarin-chalcone derivatives for the treatment of tenacibaculosis. Bioorg. Med. Chem. 23, 7045–7052.

Vekariya, R.H., Patel, H.D., 2014. Recent advances in the synthesis of coumarin derivatives via knoevenagel condensation: a review. Synth. Commun. 44, 2756–2788.

Wei, H., Ruan, J.L., Zhang, X.J., 2016. Coumarin-chalcone hybrids: promising agents with diverse pharmacological properties. Rsc Adv. 6, 10846–10860.

Wu, J.H., Wang, X.H., Yi, Y.H., Lee, K.H., 2003. Anti-AIDS agents 54. A potent anti-HIV chalcone and flavonoids from genus Desmos. Bioorg. Med. Chem. Lett. 13, 1813–1815.

Yang, J.Y., Li, X., Xue, Y., Wang, N., Liu, W.C., 2014. Anti-hepatoma activity and mechanism of corn silk polysaccharides in H22 tumor-bearing mice. Int. J. Biol. Macromol. 64, 276–280.

Yuce, B., Danis, O., Ogan, A., Sener, G., Bulut, M., Yarat, A., 2009. Antioxidative and lipid lowering effects of 7,8-dihydroxy-3-(4-methylphenyl) coumarin in hyperlipidemic rats. Arzneimittel-Forsch. 59, 129–134.

Zhan, W.H., Li, Y.Y., Huang, W.P., Zhao, Y.J., Yao, Z.L., Yu, S.Y., Yuan, S.J., Jiang, F.L., Yao, S., Li, S.X., 2012. Design, synthesis and antitumor activities of novel bis-aryl ureas derivatives as Raf kinase inhibitors. Bioorg. Med. Chem. 20, 4323–4329.

Zhang, H., Ke, J., Shao, T., Li, J., Duan, Y., He, Y., Zhang, C., Chen, G., Sun, G., Sun, X., 2014. Cytotoxic effects of procyanidins from Castanea mollissima Bl. Shell on human hepatoma G2 cells in vitro. Food Chem. Toxicol. 64, 166–176.